**Turkish Journal of Engineering**
https://dergipark.org.tr/en/pub/tuje
**e-ISSN 2587-1366**

# Interpretable AI analysis of chaos systems distribution in time series data from industrial robotics

**Cem Özkurt** *[1]

[1] *Sakarya University of Applied Sciences, Faculty of Technology, Computer Engineering, Türkiye, cemozkurt@subu.edu.tr*
[2] *Sakarya University of Applied Sciences, Artificial Intelligence and Data Science Application and Research Center, Türkiye, cemozkurt@subu.edu.tr*

Cite this study: Özkurt, C. (2024). I Interpretable AI analysis of chaos systems distribution in time series data from industrial robotics. Turkish Journal of Engineering, 8 (4), 656-665.

https://doi.org/10.31127/tuje.1471445

**Keywords**
Chaos systems
Explainable artificial Intelligence
InterpretML
Industrial robotics
Machine learning

**Research/Review Article**

Received: 20.04.2024
Revised: 25.06.2024
Accepted: 27.06.2024
Published: 31.10.2024

**Abstract**

In this study, the generalizability and distributivity of three different chaotic systems within an industrial robotics time series dataset are explored using an annotated artificial intelligence algorithm. A time series dataset derived from industrial robotics processes was constructed and transformed into the Runge-Kutta system, comprising fourth-order differential equations for normalization. Among the processed data, variables related to x-y-z positions underwent chaotic transformations through Lorenz, Chen, and Rossler chaos systems. The x variable and angle variables from the transformed x-y-z data were inputted into the InterpretML model, an annotated artificial intelligence model, to elucidate the effects of angle variables on the x position variable. As a result of this analysis, InterpretML Local analysis revealed a sensitivity of 0.05 for the Rossler chaos system, 0.15 for Chen, and 0.25 for Lorenz. Furthermore, global analysis indicated precision rates of 0.17 for Rossler, 0.255 for Chen, and 0.35 for Lorenz chaos systems. These sensitivity results suggest that the Rossler chaos system consistently provides more accurate results in both InterpretML local and global analyses compared to other chaotic systems. This study contributes significantly to the literature by analyzing the distributive and generalization properties of chaos systems and enhancing understanding of these systems.

## 1. Introduction

Chaos theory has become a powerful tool for understanding seemingly random events in nature and human-made systems. Its importance comes from its ability to explain and observe complex and unpredictable behavior. Both natural events and artificial systems, covering events ranging from changeable weather conditions against fluctuations in financial markets also helping with precision and adaptability in industrial robotics while increasing the efficiency of these systems. These chaotic events can affect the movement and performance of robot arms, impacting trajectory planning, control strategies, and overall system efficiency. Machine learning, a subfield of artificial intelligence, empowers computers to learn from data and solve complex problems iteratively. Algorithms analyze vast datasets to identify patterns and relationships, enabling them to make forecasts and support decision-making. On the other hand, Interpretable Artificial Intelligence improving the understandability of machine learning models and by providing increased performance techniques to explain their decisions. Although it is widely is used by health professionals as a reliable guide for disease diagnosis and treatment planning, but also widely used in areas such as financial analysis, market forecasting for risk assessment, In manufacturing sector. Machine learning and interpretable artificial intelligence is used to optimize production processes, quality control and can predict errors and thus improve operational efficiency. In the automotive industry, with the development of technology driver assistance systems and autonomous vehicle technologies, machine learning and interpretable artificial intelligence analyzes various sensor data and take decisions to improve driving safety and system performance. They are also used in the field of education to evaluate student performance and personalize learning processes. The study defended users' right to disclosure in algorithms affecting information privacy by presenting an interpretable AI framework for COVID-19 screening in chest X-ray, leveraging transfer learning techniques to overcome dataset limitations and achieve high diagnostic accuracy [1]. Additionally, another study aims to detect early-stage lung cancer based on machine learning methods, employing nine different algorithms including NB, LR, DT, RF, GB, and SVM. The success of the classification algorithms used was evaluated using the metrics of accuracy, sensitivity, and precision calculated using the parameters of the confusion matrix, showing that the proposed model can detect cancer with a maximum accuracy of 91% [2].

In order to test the methods proposed in this article, a data set was created using Advanced Kinematics, a robotic process, and the Runge-Kutta 4 equation (RK4). By passing the spatial x-y-z column data in this created data set through Lorenz, Chen and Rossler chaos systems, the suitability of the proposed methods to the input parameters is ensured. The effects of angle variables on the column data of the transformed x position are explained by the interpretML algorithm, an Explainable Artificial Intelligence model. In addition, the effects of the angle variables created by the robot arms in their forward kinematic movement on the converted x column data are explained with the interpretML algorithm, which is also an Explainable Artificial Intelligence model. In addition to contributing to the advancement of chaotic data analysis, the aim of the study is to explain the interaction of chaotic systems in the field of industrial robotics with machine learning and to pave the way for new applications and understandings in this interdisciplinary field.

Recent research has revealed the great potential of the intersection of machine learning (ML) techniques and chaotic systems. These techniques have been used successfully in fields ranging from quantum physics to radar and communications systems. In one study, machine learning methods were used in discoveries in quantum physics. High accuracy has been achieved to classify different regimes in single-particle and multi-particle systems. Using neural network algorithms, it has been possible to distinguish orderly and chaotic behavior in quantum billiard models [3]. Another study has shown that the standard Hidden Markov Modeling (HMM) method is effective in classifying multiple regimes in chaotic dynamical systems. Using numerical data from known chaotic systems such as Hénon and Lorenz attractors, this method has significantly increased regime classification accuracy and computational speed [4]. A study using controlled chaotic trajectories for integration in radar and communications systems provides a new solution to a significant challenge in this field. This approach allows radar and communication systems to coexist even in chaotic situations by encoding binary information and exhibits satisfactory performance in terms of bit error rate and target detection accuracy [5]. Another study extending the use of chaotic systems to the field of biomedical research investigated the application of chaotic feature extraction for gait analysis. Through the analysis of pressure sensor data and nonlinear time series, this research aims to distinguish between healthy and diseased subjects and demonstrate the potential of chaotic approaches in diagnosing balance disorders [6]. Addressed the challenge of distinguishing noise-corrupted chaotic dynamics from randomness through convolutional neural networks, while critically analyzed methods for processed food classification [7, 8]. Introduced a feature selection method amalgamating chaotic salp swarm algorithm and extreme learning machine for network intrusion detection, and proposed a novel approach for extreme learning machine regression problems [9, 10]. Curated a database of chaotic dynamical systems and discussed chaos as a benchmark for forecasting and data-driven modeling, and devised a method employing reservoir computers to classify hyperchaotic, chaotic, and regular signals [11, 12]. Explored neural networks' aptitude in classifying regular versus chaotic time series, while investigated singular value statistics of non-Hermitian random matrices for quantifying dissipative quantum chaos [13, 14]. Proposed a causality measure for extracting brain connectivity, and introduced a dataset for electromyogram signal analysis [15, 16]. Developed a prognostic model utilizing chaotic convolutional neural networks for epileptic seizure prediction, and delved into emergent topology in dissipative quantum chaos [17, 18]. Elucidated universal hard-edge statistics of non-Hermitian random matrices, while proposed an enhanced reptile search optimization with convolutional autoencoder for soil nutrient classification [19, 20]. Introduced a rapid AI model for COVID-19 diagnosis and prognosis, and discussed active learning within fractal decision boundaries [21, 22]. Lastly, expedited reinforcement learning using chaotic evolutionary computation for a driver's support display system, and advocated for a hybrid forecasting method blending machine learning with knowledge-based models [23, 24]. Employed machine learning to forecast chaotic origami dynamics, while developed a hybrid method combining HAVOK analysis and machine learning for chaotic time series prediction [25, 26]. Demonstrating the effectiveness of machine learning techniques, particularly the Extra Trees Regressor, in predicting latitude, longitude, and Haversine distance with high accuracy, the findings are supported by evaluation metrics and methodologies such as Cooks' distance outlier detection, t-SNE manifold analysis, and feature importance ranking [27].

## 2. Material and method

This section is the most important part of the article. In the narration to be made in this section, each step performed throughout the study should be specified in sufficient detail to be repeatable by someone else. In order for the scientific validity of the study to be accepted, it must be repeatable. Details that may affect the results must be conveyed.

### 2.1. Dataset used in the study

In this section, the sub-processes used during the creation of the data set are mentioned. While creating the data set, Forward Kinematics and Trajectory Planning functions, which are robotic processes, were used. Creating the data set using these two robotic processes was an important step in saving cost and time and providing a theoretical basis for the study.

#### 2.1.1. Trajectory planning

Trajectory planning functions are functions that are used very effectively, especially in the field of industrial robotics. These functions are used to plan the trajectory of the robot arm's movement in Cartesian space. Although there are many trajectory planning functions, the cubic spline trajectory planning function was used in this study for its effectiveness and interpretability. This function is essentially a polynomial function and is used to plan and interpret the orbital movement of the robotic arm.

This function, defined by the cubic spline trajectory equation:

$$q(t) = a_0 + a_1 t + a_2 t^2 + a_3 t^3 \qquad (1)$$

The variables $a_0$, $a_1$, $a_2, a_3$ in the formula 1 are coefficients that contribute to the accuracy, stability and efficiency of the actions taken in the forward kinematic movement of the robot. The potential values of these coefficients change during and after each movement of the robot arm in Cartesian space.

#### 2.1.2. Forward kinematics

There are two types of approaches in detailed transformation analysis of robotic arm movement. The first approach is the Inverse Kinematics approach and examines the transformation in a way that takes the position value as input and the angle value as the output value. The second approach is the Advanced Kinematics Approach, which uses the transformation angle value as input and examines the position value as output. In the Forward Kinematics Approach, Cartesian space is used to determine the orientation, position and orientation of the end effector of the robot arm. The Cartesian coordinates of the connection joints of the robotic arm are determined in Cartesian Space based on the angles connected to the motors. When performing Advanced Kinematics, the DH parameters method is most commonly used. This method consists of determining the essential parameters of the robot in a certain matrix and placing them in this matrix, and performing the forward kinematics process with the transformation matrix obtained. The DH parameters, key elements in this process, include link lengths ($a_i$), joint angles ($\theta_i$), link offsets ($d_i$), and the twist angles ($\alpha_i$). The modified forward kinematics formula can be expressed as follows:

$$T_{i-1}^{i} = [c\theta_i \ -s\theta_i \ 0 \ a_i \ s\theta_i c\alpha_i \ c\theta_i c\alpha_i \ -s\alpha_i \ -s\alpha_i d_i \ s\theta_i s\alpha_i \ c\theta_i s\alpha_i \ c\alpha_i \ c\alpha_i d_i \ 0 \ 0 \ 0 \ 1 \ ] \qquad (2)$$

$a_i$ : The distance between joint (i – 1) and joint i along the common normal

$\alpha_i$ : The rotation angle between joint (i - 1) and joint i, measured about the common normal, in radians

$d_i$ : The link offset between joint i – 1 and joint i along the previous z - axis

$\theta_i$ : The joint angle, representing the rotation from the $z_{i-1}$ axis tot the $z_i$ axis, in radians

Here, c and s represent cosine and sine, respectively. Utilizing this transformation matrix enabled the calculation of the numerical coordinates (x, y, z) for the robot arm's end effector as time progressed, resulting in a detailed time-series dataset.

In this study, it was aimed to create a data set on the ABB140 model industrial robot arm. Therefore, when selecting the parameters of the DH method while performing the forward kinematics process, special parameters of the ABB140 model industrial robot arm were selected. The selection of our parameters has confined our ABB140 model robotic arm within the space of our dataset. Table 1 shows the DH parameters of our ABB140 model robotic arm.

**Table 1.** DH Table of ABB140 Robot.

| $i$ | $a_i$ | $\alpha_i$ | $d_i$ | $\theta_i$ |
|---|---|---|---|---|
| 1 | 0.000 | 90 | 0.535 | $\theta_1$ |
| 2 | 0.000 | -90 | 0.000 | $\theta_2$ |
| 3 | 0.425 | 90 | 0.000 | $\theta_3$ |
| 4 | 0.392 | 0 | 0.650 | $\theta_4$ |
| 5 | 0.000 | 90 | 0.000 | $\theta_5$ |
| 6 | 0.000 | -90 | 0.110 | $\theta_6$ |

To derive the total transformation matrix from the DH parameter table, individual transformation matrices are created for each link using these parameters. The transformation matrices we create represent the spatial relationship between adjacent links in the robotic arm. By multiplying these matrices, we obtain the overall transformation matrix. The overall transformation matrix allows us to compute the end-effector position for any set of joint angles. The transformation matrices of the joints obtained using the DH table are stated in equation (3). The total transformation matrix obtained by multiplying the transformation matrices of the joints is also specified in equation (4).

$$T_0^1 = [cos\,cos\,(\theta_1) \ \ sin\,sin\,(\theta_1) \ \ 0 \ \ cos\,cos\,(\theta_1) \ - \ sin\,sin\,(\theta_1) \ \ cos\,cos\,(\theta_1) \ \ 0 \ a_1 \ sin\,sin\,(\theta_1) \ \ 0 \ 0 \ 1 \ d_1 \ 0 \ 0 \ 0 \ 1 \ ]$$

$$T_1^2 = [sin\,sin\,(\theta_2) \ \ cos\,cos\,(\theta_2) \ \ 0 \ \ sin\,a_2 sin\,(\theta_2) \ \ (\theta_2) \ \ sin\,sin\,(\theta_2) \ \ 0 \ -a_2 \ cos\,cos\,(\theta_2) \ \ 0 \ 0 \ 1 \ 0 \ 0 \ 0 \ 0 \ 1 \ ] \qquad (3)$$

$$T_2^3 = [\cos\cos(\theta_3)\ \ 0\ \ -\sin\sin(\theta_3)\ \ 0\ \sin\sin(\theta_3)\ \ 0\ \ \cos\cos(\theta_3)\ \ 0\ 0\ -1\ 0\ 0\ 0\ 0\ 0\ 0\ 1\ ]$$

$$T_3^4 = [\cos\cos(\theta_4)\ \ 0\ \ \sin\sin(\theta_4)\ \ 0\ (\theta_4)\ \ 0\ (\theta_4)\ \ 0\ 0\ 1\ 0\ d_3\ 0\ 0\ 0\ 1\ ]$$

$$T_4^5 = [(\theta_5)\ \ 0\ (\theta_5)\ \ 0\ (\theta_5)\ \ 0\ \ \cos\cos(\theta_5)\ \ 0\ 0\ 0\ 1\ 0\ 0\ 0\ 0\ 1\ ]$$

$$T_5^6 = [\cos\cos(\theta_6)\ \ (\theta_6)\ \ 0\ 0\ \ \sin\sin(\theta_6)\ \ \cos\cos(\theta_6)\ \ 0\ 0\ 0\ 0\ 1\ d_6\ 0\ 0\ 0\ 1\ ]$$

The total transformation matrix obtained by multiplying the transformation matrices of the joints is also specified in equation (4).

$$T_0^6 = [r_{11}\ r_{12}\ r_{13}\ r_{14}\ r_{21}\ r_{22}\ r_{23}\ r_{24}\ r_{31}\ r_{32}\ r_{33}\ r_{34}\ r_{41}\ r_{42}\ r_{43}\ r_{44}\ ]$$

$$\begin{aligned}
r_{11} &= \big((S_{23}C_1C_4 + S_1S_4)C_5 + S_5C_{23}C_1\big)C_6 + (S_{23}S_4C_1 - S_1C_4)S_6\\
r_{12} &= \big((S_{23}C_1C_4 + S_1S_4)C_5 + S_5C_{23}C_1\big)S_6 + (S_{23}S_4C_1 - S_1C_4)C_6\\
r_{13} &= -(S_{23}C_1C_4 + S_1S_4)S_5 + C_{23}C_1C_5\\
r_{14} &= -\big((S_{23}C_1C_4 + S_1S_4)S_5 - C_{23}C_1C_5\big)d_6 + a_1C_1 + a_2S_2C_1 + d_3C_{23}\\
r_{21} &= -\big((S_{23}S_1C_4 - C_1S_4)C_5 + S_1S_5C_{23}\big)C_6 + (S_{23}S_1S_4 + C_1C_4)S_6\\
r_{22} &= \big((S_{23}S_1C_4 - C_1S_4)C_5 + S_5C_{23}S_1\big)S_6 + (S_{23}S_4S_1 + C_1C_4)C_6\\
r_{23} &= -(S_{23}S_1C_4 - C_1S_4)S_5 + S_1C_{23}C_5\\
r_{24} &= \big((S_{23}S_1C_4 - C_1S_4)S_5 - S_1C_{23}C_5\big)d_6 + a_1S_1 + a_2S_1S_2 + d_3S_1C_{23}\\
r_{31} &= (S_{23}S_5 - C_{23}C_4C_5)C_6 + S_4S_6C_{23}\\
r_{32} &= -(S_{23}S_5 - C_{23}C_4C_5)S_6 + S_4C_{23}C_6\\
r_{33} &= -S_{23}C_5 - S_5C_{23}C_4\\
r_{34} &= (S_{23}C_5 + S_5C_{23}C_4)d_6 + a_2C_2 + d_1 - d_3S_{23}\\
r_{41} &= 0\\
r_{42} &= 0\\
r_{43} &= 0\\
r_{44} &= 1
\end{aligned} \tag{4}$$

While creating the data set, multiple robotic processes were monitored and necessary actions were taken using the information collected from the ABB140 model industrial robot arm. The process of creating the dataset is shown in Figure 1. Figure 2 shows the visualization of x-y-z data within the dataset.

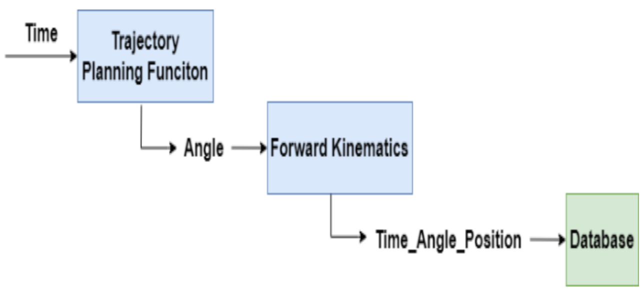


**Figure 1.** Production Flow Diagram of the Dataset.

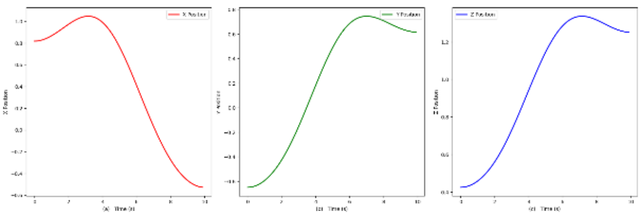

**Figure 2.** (a) End Effector's X-coordinate Over Time,(b) End Effector's Y-coordinate Over Time,(c) End Effector's Z-coordinate Over Time.

### 2.1.3. Data preprocessing

In the second stage of creating the data set produced in the study, the data set obtained as a result of robotic processes was subjected to a preprocessing operation and the data was smoothed. Runge Kutta 4 order method were used as this preprocessing operation. This method is differential equations, and thanks to these numerical operations, it is aimed to improve the accuracy of the data in the data set. The algorithm is expressed by the following formula:

$$k_1 = h.f(t_n, y_n) \tag{5}$$

$$k_2 = h.f(t_n + \frac{h}{2}, y_n + \frac{k_1}{2}) \tag{6}$$

$$k_3 = h.f(t_n + \frac{h}{2}, y_n + \frac{k_2}{2}) \tag{7}$$

$$k_4 = h.f(t_n + h, y_n + k_3) \tag{8}$$

$$y_{n+1} = y_n + \frac{1}{6}(k_1 + 2k_2 + 2k_3 + 2k_4) \tag{9}$$

In this method, the variable tn is determined as the current time, the variable yn is the current state, the variable $h$ is the time step, and the function $f(t_n, y_n)$ is determined as the derivative of the variable state 'y' according to time 't'. This method allows creating a consistent data set for further kinematics analysis by recursively calculating the current state at all time steps. In the mathematical formula, the variable $y_{n+1}$contains four more intermediate steps $(k_1, k_2, k_3, k_4)$ to help calculate the value of its future state. When examining time series, the RK4 method is used, which plays an important role in making sense of the differential equations (ODE) that create dynamic chaos systems. This method is used here due to its high efficiency and accuracy in approximating the answers of ODEs. In complex systems, RK4 finds the complexity of patterns in time series data and provides high accuracy by making strong predictions about the behavior of the system. The RK4 method, which is preferred to analyze time-changing situations in scientific applications such as robotics and dynamic system creation, provides a good balance between analysis efficiency and accuracy. This helps researchers gain in-depth information by simplifying the general understanding and prediction of the mobility of the dynamic system over time while increasing the reliability of the method. Figure 3, shows the roadmap used in preprocessing the experimental dataset. Figure 4 shows the visualization of x-y-z location data obtained from the pre-processed dataset.


**Figure 3.** Pre-Processing the Data Set.

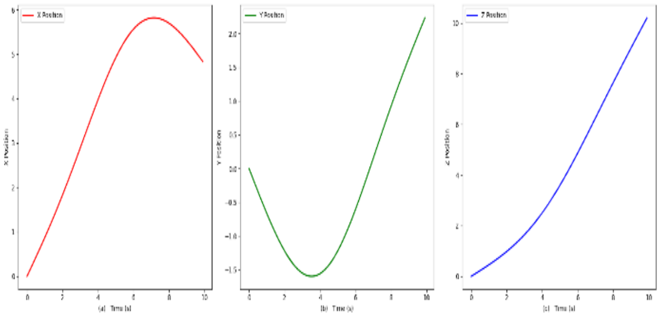

**Figure 4.** (a) Time Evolution of End Effector X Position,(b) Time Evolution of End Effector Y Position, (c) Time Evolution of End Effector Z Position.

### 2.2. Chaos system in use

#### 2.2.1. Lorenz chaos system

The emergence of the Lorenz chaotic system is considered an example of complex chaos through complex simple concepts and patterns. This chaotic system emerged as a result of Edward Lorenz's use of it in his weather forecasting studies. This system, known as the 'butterfly effect', emphasizes that phenomena obtained from small initial conditions can lead to significant consequences. This chaotic behavior is used in various fields such as meteorology, economics, seismology and neuroscience. It is also used to calculate complex and multi-parameter situations, such as measuring market fluctuations in financial terms, heart rhythm dynamics in medical terms, and population changes in social terms. Figure 5 presents graphs comparing the cross-sections of the columns of the robot arm's x, y, z positions of the new data set processed by the chaotic system with the original data set. Figure 6 shows the relational graphics of the data in the columns of x-y, y-z and x-z position change in the data set where the chaotic system is processed. The Lorenz system is governed by ordinary differential equations (ODEs), which generate the following data set:

$$\frac{dt}{dt} = \sigma(y - x) \tag{10}$$

$$\frac{dy}{dt} = x(p - z) - y \tag{11}$$

$$\frac{dz}{dt} = xy - \beta z \tag{12}$$

$\sigma$ : Prandtl number defines it as a function of the viscosity of the fluid depending on its thermal conductivity.

$\rho$ : Rayleigh number is defined as the relationship of the liquid layer with temperature.

$\beta$ : Geometric factor, finds the effect of the ratios consisting of the horizontal and vertical dimensions of the convection cell on the system.

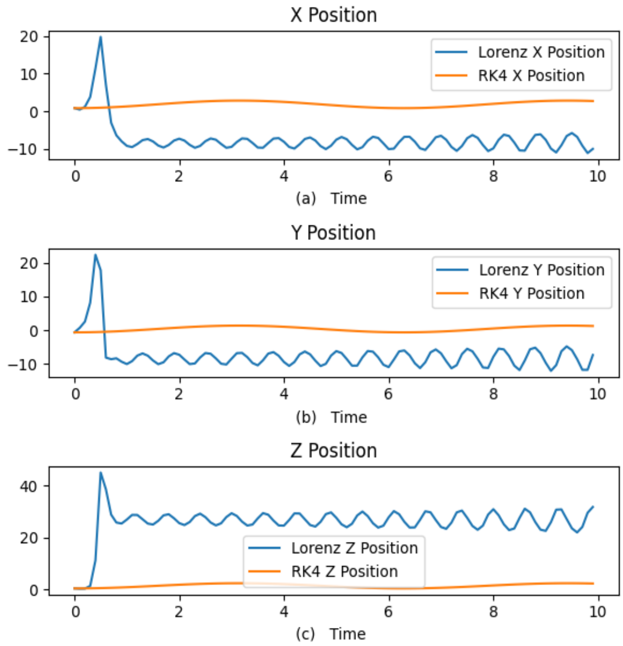


**Figure 5.** (a) RK4-Lorenz X-coordinate Trajectories,(b) RK4-Lorenz Y-coordinate Trajectories,(c) RK4-Lorenz Z-coordinate Trajectories.

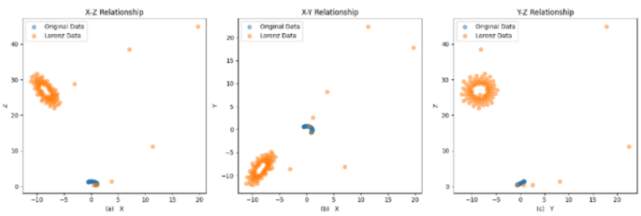

**Figure 6.** (a) Original-Lorenz X-Z Relationship,(b) Original-Lorenz X-Y Relationship,(c) OriginalLorenz Y-Z Relationship.

#### 2.2.2. Chen chaos system

The Chen chaos system is a valuable tool for modeling complex systems, particularly those exhibiting chaotic and unpredictable behavior. Chaos inherently disrupts order, making it challenging to understand and predict these systems dynamics. The Chen system tackles this challenge by unraveling the complexities and providing insights into their behavior. Its versatility extends to various fields, including weather forecasting, financial market analysis, and population dynamics, where it helps evaluate future trends and potential scenarios. The Chen chaos system plays a critical role in solving real-world problems by combining computer simulations, mathematical modeling, and data analysis techniques.

Figures 7 and 8 visually describe the system's impact. Figure 7 compares the original dataset (x-yz columns) with the post-implementation data (x, y, z columns) extracted after applying the Chen system. Figure 8 utilizes relational graphs to showcase the interdependencies between data points (x-y, y-z, and x-z) processed through the system. The specific mathematical formulation of the Chen system involves three sets of Ordinary Differential Equations, which will be discussed in the following section.

$$\frac{dx}{dt} = a(x - y) \quad (13)$$

$$\frac{dx}{dt} = (c - a)x - xz + cy \quad (14)$$

$$\frac{dz}{dt} = xy - bz \quad (15)$$

$a$ : A parameter that controls the change in the evolution rate of the system.

$b$ : A parameter affecting the nonlinearity of the system.

$c$ : A parameter influencing the coupling between variables.

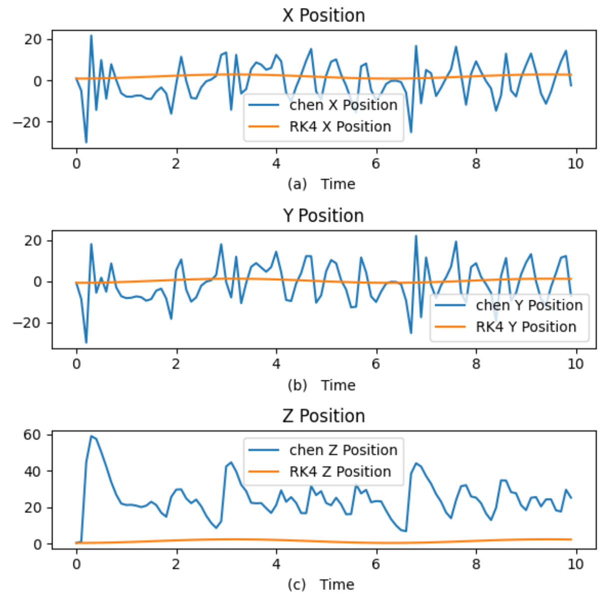


**Figure 7.** (a) RK4-Chen X Positions,(b) RK4-Chen Y Positions,(c) RK4-Chen Z Positions.

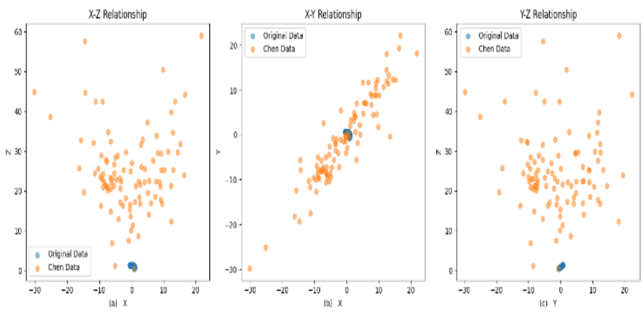


**Figure 8.** (a) Original-Chen X-Z Relationship,(b) Original-Chen X-Y Relationship,(c) Original-Chen Y-Z Relationship.

### 2.2.3. Rossler Chaos System

The Rossler chaos system consists of a set of differential equations to determine chaotic behavior. This system was designed by Edward Lorenz during a study to model the chaotic behavior of weather. This system, which is a 3D dynamic workspace, offers the most concrete example of the chaotic behavior created by variable parameters. Therefore, it is known as the most important system of chaos theory. Randomness provides a fundamental model for research and analysis in many physical, biological and engineering applications, especially signal processing and cryptography.

Figure 9 shows the comparison of the x, y, z values of our new data set after applying the Rossler chaos system to the x, y, z values in our data set. Figure 10 shows the correlations between x-, y-z and x-z values obtained after the Rossler chaos system we applied to our data set.

The differential equations that make up the Rossler chaos system are as follows:

$$\frac{dx}{dt} = -y - z \quad (16)$$

$$\frac{dy}{dt} = x + ay \quad (17)$$

$$\frac{dz}{dt} = b + z(x - c) \quad (18)$$

$a$ : A parameter determining the strength of the nonlinear term in the y equation.

$b$ : A parameter affecting the linear term in the z equation.

$c$ : A parameter influencing the nonlinear term in the z equation.

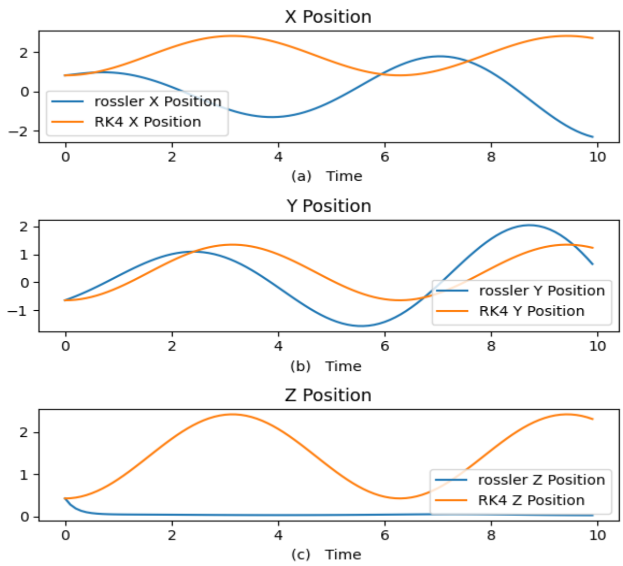


**Figure 9.** (a) RK4-Rossler X Positions,(b) RK4-Rossler Y Positions,(c) RK4-Rossler Z Positions.

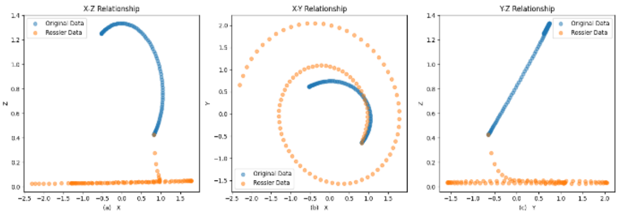

**Figure 10.** (a) Original-Rossler X-Z Relationship,(b) Original-Rossler X-Z Relationship,(c) OriginalRossler Y-Z Relationship.

### 2.3. Interpretable AI model in use

Interpretable AI stands out as a field of research that aims to explain the inner workings of complex artificial intelligence models and make them understandable by humans. This approach uses features or attributes that can be understood and accurately expressed to explain algorithm-based decision processes that are traditionally difficult to understand. This way, the model's decisions can be accessed reliably while gaining a deeper understanding of how the model works. It is important to ensure reliability by increasing the transparency of decision processes, especially in critical application areas such as medical diagnoses, legal decisions and financial analyses.Insufficient interpretability of machine learning models used in healthcare may impede data-driven decision-making in the healthcare sector [28]. In the study definitions, nuances, challenges,and requirements for the design of interpretable machine learning models in healthcare are extensively discussed; furthermore, various uses of these models in healthcare and the selection of the appropriate interpretable machine learning algorithm for a given problem are addressed. Figure 6 shows the output of an interpretML model showing the importance of the "Native Country" attribute in different countries. The model predicted that this feature had the highest importance in the first country and the lowest importance in the second country.

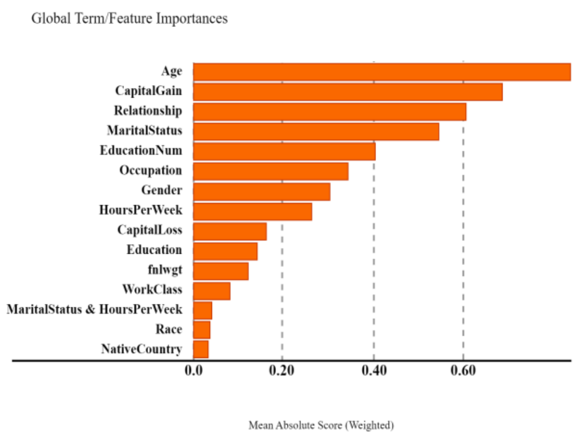


**Figure 11.** InterpretML Analysis Report.

## 3. Results

In this study, an angle-position data set of an industrial robot arm was created by using the advanced kinematics formulae of the robot arm. The position variable X in the generated data set was transformed by Lorenz, Chen and Rossler chaos systems. The transformed X position variable and the angle variables in the data set were explained with InterpretML, an Interpreted Artificial Intelligence model.

In Figure 12, the global explanation of the effects of Joint Angle 1, Joint Angle 2, Joint Angle 3, Joint Angle 4, Joint Angle 5, Joint Angle 6 variables in the data set on the X position variable passed through the Lorenz chaos system with InterpretML is visualized. Joint Angle 1 variable 0.1, Joint Angle 2 variable 0.088, Joint Angle 3 variable 0.087, Joint Angle 4 variable 0.086, Joint Angle 5 variable 0.085, Joint Angle 6 variable 0.085, Joint Angle 6 variable 0.084, binary angles have almost 0 weighted effect on Lorenz X position variable. As a result of these weighted effects, it is observed that Joint Angle 1 has the most effect on Lorenz X position and Joint Angle 6 has the least effect.

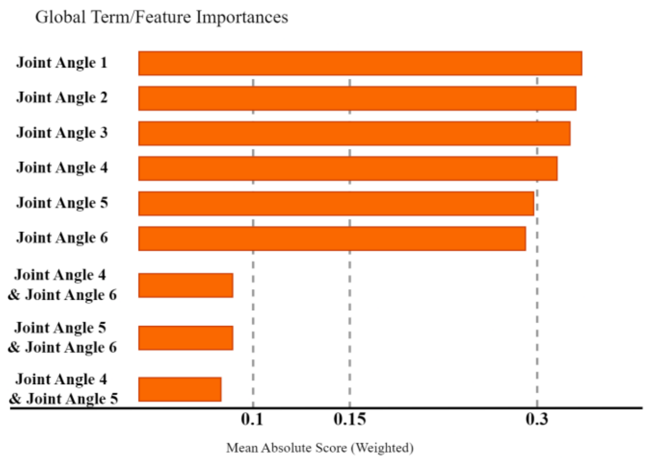


**Figure 12.** InterpretML Global Analysis for Lorenz X Position.

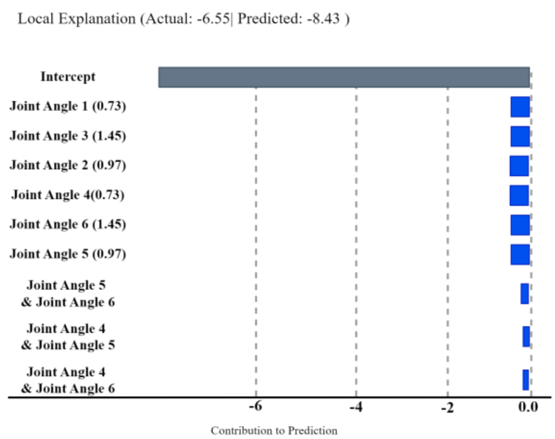


**Figure 13.** InterpretML Local Analysis for Lorenz X Position.

In Figure 13, the local explanation of the effects of Joint Angle 1, Joint Angle 2, Joint Angle 3, Joint Angle 4, Joint Angle 5, Joint Angle 6 variables in the data set on the X position variable passed through the Lorenz chaos system with InterpretML is visualized. Joint Angle 1 variable -0.73, Joint Angle 2 variable -0.97, Joint Angle 3 variable -1.45, Joint Angle 4 variable -0.73, Joint Angle 5 variable -0.97, Joint Angle 6 variable -1.45, binary angles have almost 0 weighted effect on Lorenz X position variable. As a result of these weighted effects, it is observed that Joint Angle 3 and Joint Angle 6 variables have the highest negative effect on Lorenz X position, while Joint Angle 1 and Joint Angle 4 variables have the least effect.

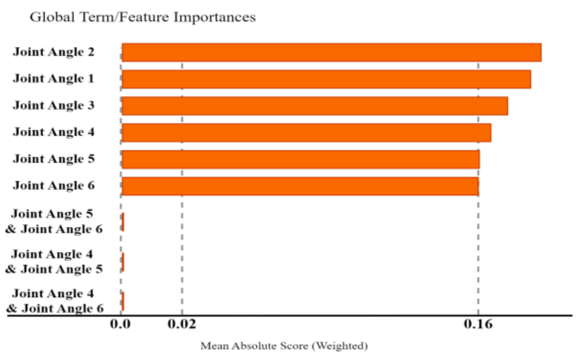


**Figure 14.** InterpretML Global Analysis for Rossler X Position.

In Figure 14, the global explanation of the effects of Joint Angle 1, Joint Angle 2, Joint Angle 3, Joint Angle 4, Joint Angle 5, Joint Angle 6 variables in the data set on the X position variable passed through the Rossler chaos system with InterpretML is visualized. Joint Angle 1 variable 0.168, Joint Angle 2 variable 0.17, Joint Angle 3 variable 0.165, Joint Angle 4 variable 0.162, Joint Angle 5 variable 0.16, Joint Angle 6 variable 0.16, Joint Angle 6 variable 0.084, binary angles have almost 0 weighted effect on Rossler X position variable. As a result of these weighted effects, it is observed that Joint Angle 2 has the most effect on Lorenz X position and Joint Angle 5 and Joint Angle 6 has the least effect.

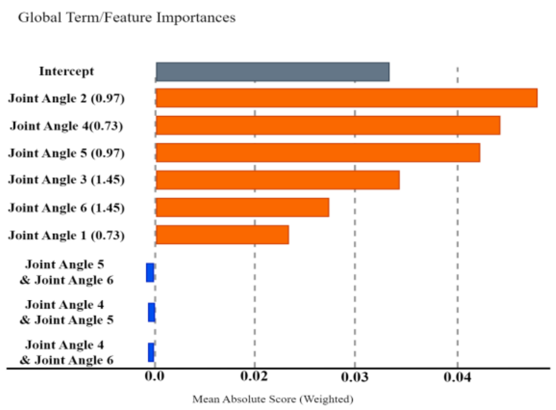


**Figure 15.** InterpretML Local Analysis for Rossler X Position.

In Figure 15, the local explanation of the effects of Joint Angle 1, Joint Angle 2, Joint Angle 3, Joint Angle 4, Joint Angle 5, Joint Angle 6 variables in the data set on the X position variable passed through the Rossler chaos system with InterpretML is visualized. Joint Angle 1 variable 0.023, Joint Angle 2 variable 0.05, Joint Angle 3 variable 0.033, Joint Angle 4 variable 0.045, Joint Angle 5 variable 0.028, Joint Angle 6 variable -1.45, binary angles have almost 0 weighted effect on Rossler X position variable. As a result of these weighted effects, it is observed that Joint Angle 2 variable have the highest positive effect on Lorenz X position, while Joint Angle 1 variable have the least effect.

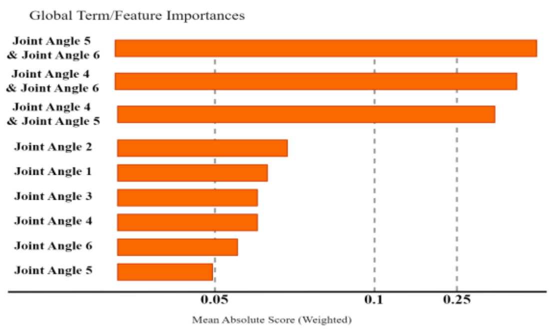


**Figure 16.** InterpretML Global Analysis for Chen X Position.

In Figure 16, the global explanation of the effects of Joint Angle 1, Joint Angle 2, Joint Angle 3, Joint Angle 4, Joint Angle 5, Joint Angle 6 variables in the data set on the X position variable passed through the Chen chaos system with InterpretML is visualized. Joint Angle 1 variable variable 0.053, Joint Angle 2 variable variable 0.057, Joint Angle 3 variable 0.052, Joint Angle 4 variable variable 0.052, Joint Angle 5 variable 0.047, Joint Angle 6 variable 0.051, Joint Angle 5-6 0.28, Joint Angle 4-6 0.273,Joint Angle 4-5 0.27 have weighted effect on Chen X position variable. As a result of these weighted effects, it is observed that Joint Joint Angle 5-6 has the most effect on Chen X position and Joint Angle 5 has the least effect.

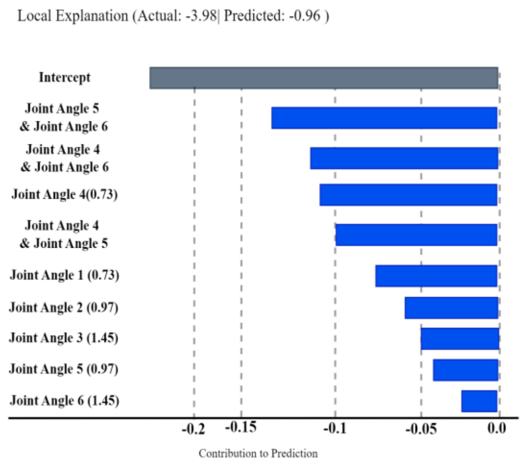


**Figure 17.** InterpretML Local Analysis for Chen X Position.

In Figure 17, the local explanation of the effects of Joint Angle 1, Joint Angle 2, Joint Angle 3, Joint Angle 4, Joint Angle 5, Joint Angle 6 variables in the data set on the X position variable passed through the Chen chaos system with InterpretML is visualized. Joint Angle 1 variable -0.09, Joint Angle 2 variable -0.07, Joint Angle 3 variable -0.05, Joint Angle 4 variable -0.11, Joint Angle 5 variable -0.045, Joint Angle 6 variable -0.045,Joint Angle 4-5 -0.1, Joint Angle 4-6 -0.105 and Joint Angle 5-6 -0.125 weighted effect on Chen X position variable. As a result of these weighted effects, it is observed that Joint Angle 5-6 have the highest negative effect on Chen X position, while Joint Angle 6 variable have the least effect.

## 4. Discussion

As a result of this study, it has been shown that time series data of chaos systems can be used successfully to improve the learning ability. The time series data set of the ABB140 model industrial robot was processed with three different chaos systems: Lorenz, Rossler and Chen, and significant improvements were observed in the understandability and interpretability of the data set. The transformations created with this chaos system provided important information about the relationship between the position variable X and the angle variables.

The InterpretML model, an explainable artificial intelligence model, was used to detect the effects of angles on the transformed X position data. Results found with InterpretML showed that it is robust in both global and local analysis; Its compatibility with the Rossler chaos system has been determined. These results have been observed in the role of advanced interpretability techniques such as InterpretML to extract useful information from complex data sets generated by chaotic models. By comparing the usability of OmniXAI and InterpretML integrated frameworks in the healthcare industry and in terms of explaining the models' predictions, Yu found that InterpretML explained its data more accurately [29].

A contribution to the existing literature is made by emphasizing the importance of chaos systems in increasing the interpretability of machine learning models, especially in areas such as robotics and industrial automation. By exploiting the inherent dynamics of chaotic systems, not only the learning capabilities of our model were improved, but also the distributional relationships of chaos systems were revealed and their efficiency regarding their applicability in data analysis and prediction was demonstrated. Abdul Karim advocates a shift towards a question-based approach to interpretability in machine learning, emphasizing the importance of addressing specific questions about interpretability rather than focusing solely on the tools used, thereby encouraging a deeper understanding of machine learning not just as a science. It is just an engineering application [30].

## 5. Conclusion

In this study, the chaos distribution on the industrial robot data set was tried to be explained with annotated artificial intelligence. Advanced kinematics and trajectory planning functions were used when designing the data set, and thus the first versions of the data set were created. The obtained data set was pre-processed with the Runge Kutta 4 method and the data set we will mainly use was created. The created original data set was passed through 3 different chaos systems and the effects of the angle variables in the data set on the position variable X were explained in detail with Annotated Artificial Intelligence. In the updated data set, the data of x, y and z position variables were transformed by passing through these 3 chaos systems: Lorenz, Rossler and Chen. The effects of angles on the transformed X position data are explained with the InterpretML model, which is an Explanatory Artificial Intelligence model. As a result of the explanation, InterpretML explained the local analysis for the Rossler chaos system with 0.05, Chen 0.15 and Lorenz 0.25 precision; Global analysis for Rossler chaos system with precision of 0.17, Chen with precision of 0.255 and Lorenz with precision of 0.35. According to these precise results, InterpretML is more consistent in local and global analysis because the Rossler chaos system gives more accurate results than other chaos systems. This study sheds light on the importance and explanation of the distributiveness of chaos systems.

In the future, as the functionality of integrating chaos theory into machine learning methodologies is seen, it will create new possibilities in data-driven decision-making in various fields. Future research efforts are expected to be directed towards integrating insights from chaos theory to improve the interpretability of machine learning models and facilitate the development of more robust and effective predictive models. Chun Zhang argues for the necessity of integrating chaos theory with machine learning. This integration may enable the development of new and powerful tools for data-driven decision-making in various fields in the future. Future research is expected to use insights from chaos theory to help improve the interpretability of machine learning models and create more robust and effective predictive models [31].

**Acknowledgement**

The author would like to thank all the data sets, materials, information sharing and support used in the assembly of this article.

**Author contributions**

The author wrote and reviewed the article.

**Conflicts of interest**

The author declare that he has no known competing financial interests or personal relationships that could have appeared to influence the work reported in this paper.

**References**

1. Tsiknakis, N., Trivizakis, E., Vassalou, E. E., Papadakis, G. Z., Spandidos, D. A., Tsatsakis, A., Sánchez-García, J., López-González, R., Papanikolaou, N., Karantanas, A. H., & Marias, K. (2020). Interpretable artificial intelligence framework for covid-19 screening on chest x-rays. *Experimental and Therapeutic Medicine, 20*(2), 1351–1357.
2. Dirik, M. (2023). Machine learning-based lung cancer diagnosis. *Turkish Journal of Engineering, 7*(4), 322-330. https://doi.org/10.31127/tuje.1180931
3. Kharkov, Y. A., Sotskov, V. E., Karazeev, A. A., Kiktenko, E. O., & Fedorov, A. K. (2019). Revealing quantum chaos with machine learning. *arXiv-quant-ph.*

4. Bhattacharya, C., & Ray, A. (2020). Data-driven detection and classification of regimes in chaotic systems via hidden Markov modeling. *Unknown.*
5. Pappu, C. S., Carroll, T. L., & Flores, B. C. (2020). Simultaneous radar-communication systems using controlled chaos-based frequency modulated waveforms. *IEEE Access.*
6. Ikizoglu, S., & Atasoy, B. (2020). Chaotic approach based feature extraction to implement in gait analysis. *Unknown.*
7. Mukhopadhyay, S., & Banerjee, S. (2020). Learning dynamical systems in noise using convolutional neural networks. *Chaos (Woodbury, N.Y.).*
8. Sadler, C. R., Grassby, T., Hart, K., Raats, M. M., Soković, M., & Timotijevic, L. (2021). Processed food classification: Conceptualisation and challenges. *Trends in Food Science and Technology.*
9. Hadi, R. N., Mahmoud, R. O., & Tag Eldien, A. S. (2021). Feature selection method based on chaotic salp swarm algorithm and extreme learning machine for network intrusion detection systems. *WeboLogy.*
10. Altay, O., Ulas, M., & Alyamac, K. E. (2021). Dcs-elm: A novel method for extreme learning machine for regression problems and a new approach for the sfrscc. *PeerJ. Computer Science.*
11. Gilpin, W. (2021). Chaos as an interpretable benchmark for forecasting and data-driven modelling. *arXiv-cs.LG.*
12. Liedji, D. W., & Mbé, J. H. T., Kenne, G. (2023). Classification of hyperchaotic, chaotic, and regular signals using single nonlinear node delay-based reservoir computers. *Chaos (Woodbury, N.Y.).*
13. Corbetta, A., & Jong, T. G. (2023). How neural networks learn to classify chaotic time series. *Chaos (Woodbury, N.Y.).*
14. Kawabata, K., Xiao, Z., Ohtsuki, T., & Shindou, R. (2023). Singular-value statistics of non-Hermitian random matrices and open quantum systems. *arXiv-cond-mat.mes-hall.*
15. Avvaru, S., & Parhi, K. K. (2023). Effective brain connectivity extraction by frequency domain convergent cross-mapping (FDCCM) and its application in Parkinson's disease classification. *IEEE Transactions on Biomedical Engineering.*
16. Khodadadi, V., Rahatabad, F. N., Sheikhani, A., & Dabanloo, N. J. (2023). A dataset of a stimulated biceps muscle of electromyogram signal by using Rossler chaotic equation. *Data in Brief.*
17. Palanisamy, P., Urooj, S., Arunachalam, R., & Lay-Ekuakille, A. (2023). A novel prognostic model using chaotic CNN with hybridized spoofing for enhancing diagnostic accuracy in epileptic seizure prediction. *Diagnostics (Basel, Switzerland).*
18. García-García, A. M., Sá, L., Verbaarschot, J. J. M., & Yin, C. (2023). Emergent topology in many-body dissipative quantum chaos. *arXiv-cond-mat.str-el.*
19. Xiao, Z., & Shindou, R. (2024). Universal hard-edge statistics of non-Hermitian random matrices. *arXiv-cond-mat.mes-hall.*
20. Raman, P., & Chelliah, B. J. (2023). Enhanced reptile search optimization with convolutional autoencoder for soil nutrient classification model. *PeerJ.*
21. Huyut, M. T., & Velichko, A. (2023). Lognnet model as a fast, simple and economical AI instrument in the diagnosis and prognosis of covid-19. *MethodsX.*
22. Payot, N., Pasquato, M., Travan, A., Marsili, E., & Bianconi, G. (2023). Active learning in fractal decision boundaries. *arXiv-cs.LG.*
23. Yamaguchi, T., Takahashi, H., Nakagawa, Y., & Arai, T. (2001). Speeding up reinforcement learning using chaotic evolutionary computation for a driver's support display system. *Unknown.*
24. Pathak, J., Hunt, B. R., Girvan, M., Lu, Z., & Ott, E. (2018). Model-free prediction of large spatiotemporally chaotic systems from data: A hybrid multiple model framework. *Chaos (Woodbury, N.Y.).*
25. Yasuda, K., Matsumoto, Y., Iwata, K., & Hasegawa, T. (2020). Data-driven modeling for chaotic origami dynamics prediction with machine learning. *Unknown.*
26. Yang, Y., Huang, D.-S., Huang, H., Guo, J.-Y., Li, Y., & Fang, H. (2022). Hybrid method using Havok analysis and machine learning for chaotic time series prediction. *IEEE Access.*
27. Mogaraju, J. K. (2024). Machine learning empowered prediction of geolocation using groundwater quality variables over YSR district of India. *Turkish Journal of Engineering, 8*(1), 31-45. https://doi.org/10.31127/tuje.1223779
28. Abdullah, T. A. A., Zahid, M. S. M., & Ali, W. (2021). A review of interpretable ML in healthcare: Taxonomy, applications, challenges, and future directions. *Symmetry, 13*, 2439. https://doi.org/10.3390/sym13122439
29. Yu, H. Q., Alaba, A., & Eziefuna, E. (2024). Evaluation of integrated XAI frameworks for explaining disease prediction models in healthcare. In: Qi, J., & Yang, P. (Eds.) *Internet of Things of Big Data for Healthcare. IoTBDH 2023. Communications in Computer and Information Science, vol 2019.* Springer, Cham. https://doi.org/10.1007/978-3-031-52216-1_2
30. Karim, A., Mishra, A., Newton, M. A., & Sattar, A. (2018). Machine learning interpretability: A science rather than a tool. *arXiv preprint arXiv:1807.06722.*
31. Zhang, C., Jiang, J., Qu, S.-X., & Lai, Y.-C. (2020). Predicting phase and sensing phase coherence in chaotic systems with machine learning. *Chaos, 30*(8), 083114.